tember to 5 November 1976. The lander 2 primary mission ended on 5 November 1976, just before conjunction. A total of about 450 images were acquired by lander 1 and about 575 images by lander 2. The imagery was divided among high-resolution composites, normal color composites, seven-channel spectrophotometric composites, atmospheric and surface experiments, sample support imagery, and imagery to support physical and magnetic properties experiments. With the advent of the extended mission, lander imagery experiments aimed at monitoring changes in atmospheric properties and surface features will be implemented in order to understand Mars as it varies through the seasons.

T. A. Mutch, S. U. Grenander
K. L. Jones, W. Patterson
Department of Geological Sciences,
Brown University,
Providence, Rhode Island 02912
R. E. Arvidson
E. A. Guinness
McDonnell Center for the Space
Sciences, Department of Earth and
Planetary Sciences, Washington
University, St. Louis, Missouri 63130
P. Avrin
C. E. Carlston
Martin Marietta Corporation,
Denver, Colorado 80201
A. B. Binder
Institut für Geophysik, University of
Kiel, Federal Republic of Germany, and
Science Applications, Inc.,
Pasadena, California 91101
C. Sagan, E. W. Dunham
P. L. Fox, D. C. Pieri
Laboratory for Planetary Studies,
Cornell University,
Ithaca, New York 14853
F. O. Huck, C. W. Rowland
G. R. Taylor, S. D. Wall
NASA Langley Research Center,
Hampton, Virginia 23665
R. Kahn
Center for Earth and Planetary
Physics, Harvard University,
Cambridge, Massachusetts 02138
E. C. Levinthal, S. Liebes, Jr.
R. B. Tucker
Department of Genetics, School of
Medicine, Stanford University,
Stanford, California 94305
E. C. Morris
U.S. Geological Survey,
Flagstaff, Arizona 86001
J. B. Pollack
NASA Ames Research Center,
Moffett Field, California 94305
R. S. Saunders, M. R. Wolf
Jet Propulsion Laboratory,
Pasadena, California 91103

References and Notes

1. H. Masursky and N. L. Crabill, *Science* **194**, 62 (1976).
2. L. Soderblom, T. Kreidler, H. Masursky, *J. Geophys. Res.* **78**, 4117 (1973).
3. T. A. Mutch, A. B. Binder, F. O. Huck, E. C. Levinthal, S. Liebes, Jr., E. C. Morris, W. R. Patterson, J. B. Pollack, C. Sagan, G. R. Taylor, *Science* **193**, 791 (1976).
4. F. O. Huck, H. F. McCall, W. R. Patterson, G. R. Taylor, *Space Science Instrum.* **1**, 189 (1975).
5. In addition to corrections for lander tilt, each image was processed to remove geometric distortions related to use of high-resolution photodiodes that are located at different locations on the camera's photosensor array.
6. Block counts were made from the lander 2 sol 0 camera 2 survey image for a region extending 15 m in front of the spacecraft. More refined block counts reduced by computer processing of stereo pairs will appear in a forthcoming paper.
7. H. Blatt, G. Middleton, R. Murray, *Origin of Sedimentary Rocks* (Prentice-Hall, Englewood Cliffs, N.J., 1972).
8. T. A. Mutch, R. E. Arvidson, A. B. Binder, F. O. Huck, E. C. Levinthal, S. Liebes, Jr., E. C. Morris, D. Nummedal, J. B. Pollack, C. Sagan, *Science* **194**, 87 (1976). The 100-μm upper limit on particle size is an inference, since the pixel size on the surface at optimum focus is about 1 mm. The inference is based on (i) the mechanical behavior of material exposed in trenches [R. W. Shorthill, H. J. Moore, II, R. F. Scott, R. E. Hutton, S. Liebes, Jr., C. R. Spitzer, *Science* **194**, 91 (1976)], and (ii) the observation that at both sites the fines seem to be dominated by clay minerals (*13*), which are characteristically fine-grained.
9. C. Sagan, in preparation.
10. J. Jaeger, *Am. J. Sci.* **259**, 721 (1961).
11. A. Lachenbruch, *Geological Society of America Special Paper No. 70* (1962).
12. F. Wade and J. DeWys, *Icarus* **9**, 175 (1968).
13. A. K. Baird, P. Toulmin, B. C. Clark, H. J. Rose, Jr., K. Keil, R. P. Christian, J. L. Gooding, *Science* **194**, 1288 (1976).
14. J. Neal, A. Langer, P. Kerr. *Geol. Soc. Am. Bull.* **79**, 69 (1968).
15. R. Grim, *Applied Clay Mineralogy* (McGraw-Hill, New York, 1962).
16. A large number of people have contributed to the success of the Viking mission. In particular our thanks go to the Viking management, to the lander mission planning groups, and to the analysts at the Image Processing Laboratory at the Jet Propulsion Laboratory. We are also most grateful to the group of undergraduate students who worked on various phases of lander imagery as part of the Viking intern program, supported by the Planetology Program Office, NASA Headquarters, and by the Alfred P. Sloan Foundation. This research was supported by NASA.

15 November 1976

Inorganic Analyses of Martian Surface Samples at the Viking Landing Sites

Abstract. *Elemental analyses of fines in the Martian regolith at two widely separated landing sites, Chryse Planitia and Utopia Planitia, produced remarkably similar results. At both sites, the uppermost regolith contains abundant Si and Fe, with significant concentrations of Mg, Al, S, Ca, and Ti. The S concentration is one to two orders of magnitude higher, and K (< 0.25 percent by weight) is at least 5 times lower than the average for the earth's crust. The trace elements Sr, Y, and possibly Zr, have been detected at concentrations near or below 100 parts per million. Pebble-sized fragments sampled at Chryse contain more S than the bulk fines, and are thought to be pieces of a sulfate-cemented duricrust.*

Each Viking lander carries an energy-dispersive x-ray fluorescence spectrometer (XRFS) for elemental analysis of samples of the martian surface. The design characteristics and expected performance capabilities for this instrument have been described elsewhere (*1*). In an earlier report, we presented preliminary results of the first analysis of fines in situ at Chryse Planitia (*2*). Although data collection and reduction are still in progress, we present in Tables 1 and 2 our interim results of the analyses accomplished to date.

Analysis methods. Because of the weight constraints on the Viking pay-

Table 1. Element abundances in Mars samples. Concentrations are expressed as percentages by weight. NA indicates that data are not yet available.

Element	S1	S2 minus S1	S3 minus S1*	U1 minus S1
Mg	5.0 ± 2.5	NA	+0.2	NA
Al	3.0 ± 0.9	NA	−0.1	NA
Si	20.9 ± 2.5	−0.1	−0.4	−0.9
S	3.1 ± 0.5	+0.7	+0.7	−0.5
Cl	0.7 ± 0.3	+0.1	+0.2	−0.1
K	<0.25	0	0	0
Ca	4.0 ± 0.8	−0.2	0	−0.4
Ti	0.51 ± 0.2	0	0	+0.1
Fe	12.7 ± 2.0	−0.1	+0.4*	+1.5
"O"†	50.1 ± 4.3	NA	NA	NA
X†	8.4 ± 7.8	NA	NA	NA

*All S3 concentrations have been adjusted by a preliminary correction factor of 0.9 to compensate the effect of a partial fill on the analysis. The Fe is also affected by the contribution of ^{55}Fe to the peak. Trace elements analyze low. †"Oxygen" is the sum of all elements not directly determined. If the detected elements are all present as their common oxides (Cl excepted), then *X* is the sum of nondetected components, including H_2O, Na_2O, CO_2, and NO_x.

load, the design of the electronics in the XRFS is such that repeated spectral scans over several days of operation are necessary to obtain statistically adequate data. Multivariate analysis of the computed means of prominent peaks allows separation and correction for time- and temperature-dependent components of gain change. The three techniques used to provide independent evaluations of the absolute energy scale have been described (*2*). Each instrument was calibrated by reference to spectra of 25 solid rock and mineral prisms measured just prior to being installed in the spacecraft. Detailed compositions have been determined for powders from chips of the same rock prisms, but the prism faces themselves must also be analyzed because of the inhomogeneous nature of some of them. These analyses are now under way for the three prisms currently used for reduction of the Mars results, namely a black shale (our reference No. 8066), a biotite peridotite (8064), and a syenogabbro (8063). The first of these is used primarily as a standard for sulfur concentration; for elements other than sulfur, the analytical results presented here are based on a compromise between 8063 and 8064. For the present report, the background level from the lander's plutonium-fueled power sources (radioisotope thermoelectric generators) is determined from the proportional counter No. 2 (PC2) spectrum taken just after landing, and the PC1, PC3, PC4 levels are scaled from the known characteristics of this interference. More detailed analysis of PC1 spectra will improve the background correction. Continuing data analysis is expected to refine the results for most elements, especially for Mg, Al, Si, and the apparently minor, but very important constituents K and Cl. All analytical results assume homogeneity for each martian sample.

Table 2. Trace element abundances at two sites on Mars, expressed as parts per million.

Element	S1	U1
Rb	≤30	≤30
Sr	60 ± 30	100 ± 40
Y	70 ± 30	50 ± 30
Zr	≤30	30 ± 20

Results for sample 1. The most abundant element detected is silicon. Expressed as SiO_2, it accounts for 45 ± 5 percent by weight of the martian fines at Chryse (sample S1), in agreement with our previous conclusion that silicate minerals constitute a major fraction of the total sample (*2*). This value is lower than the 60 ± 10 percent SiO_2 previously inferred (*3*) from orbital infrared spectroscopy of suspended material during the 1971 dust storm. The overall pattern of element concentrations appears unlike any simple major rock or soil unit known on either Earth or Moon. The concentration of S is high, while the concentrations of Al and the trace elements are low. The relative abundances of some elements approximate those found in stony meteorites, but the Al/Si and Ti/Fe ratios are both significantly higher than in chondritic meteorites, and S is higher than in achondrites. The mineralogic implications of the chemical results are discussed by Baird *et al.* (*4*).

Table 3. Upper limits established for elements other than those in Tables 1 and 2 in the Mars samples.

Elements not detected	Detection limit (%)	Interfering emissions
Mn, Co, Ni	2	Fe
Cu, Zn, Ga	1	Fe
Ge, As, Se, Br	0.1	
Nb, Mo, Tc	0.01	
Ru, Rh, Pd	0.03	
Ag, Cd, In	0.5	Cl, K
Sn, Sb, Te, I	4	Ca
Cs, Ba, La, Ce	0.5	Ti
Pr to Hf	5	Fe
Ta, W, Re, Os, Ir	1	Fe
Pt, Au, Hg, Pb, Bi to Fr	0.1	
Ra, Ac, Th, Pa, U	0.01	Sr, Y

In Fig. 1, the cumulative pooled spectra from PC4 are shown for the trace element energy range, before and after stripping out the backscatter peak and its low-energy tail. The presence of Sr and Y appears certain, Zr probable, while Rb and Mo are apparently at concentrations below the XRFS minimum detection limit (*1*). Table 3 lists the upper limits for other elements not detected. It should be added that these elements were not expected to be present at detectable levels on the basis of general geochemical considerations. In some instances, interference was caused by a detected element masking the instrumental sensitivity limit for a noninterfering matrix. Those elements causing such interference are indicated in Table 3.

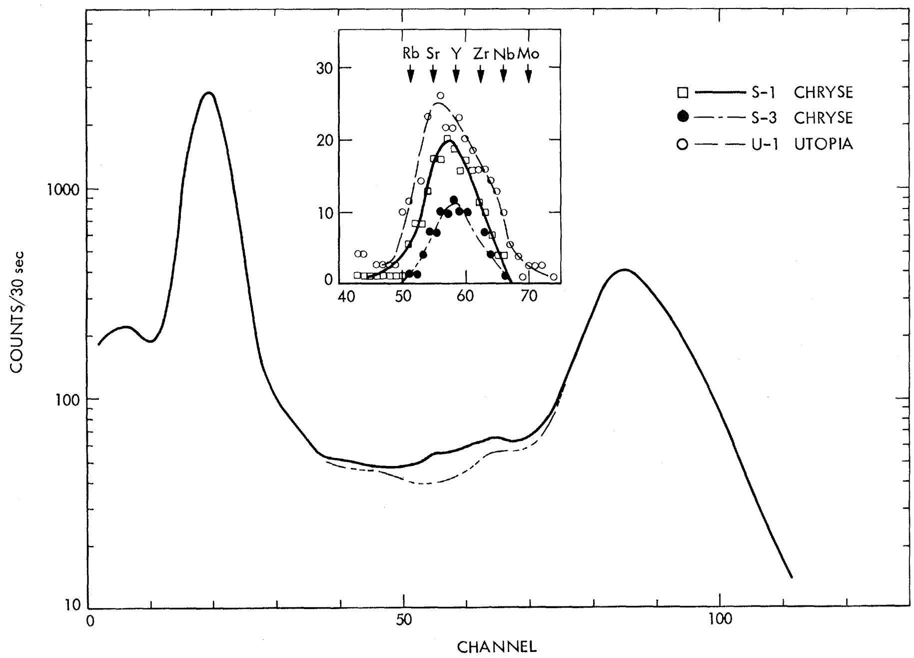

Fig. 1. Data from detector PC4. The solid curve shows pooled data for the first sample at Chryse (S1). The dashed curve shows the spectrum expected in the absence of emissions in the trace element range. The inset shows a linear graph of samples S1, S3, and the first sample from the Utopia site, U1, with the dashed curve stripped out to reveal trace-element peaks.

Sulfur. A most striking finding is the high concentration of S in the martian fines. This is some 10 to 100 times higher than in common terrestrial (*5, 6*) and lunar (*7*) rocks and soils, but about the same magnitude as many chondritic meteorites, widely regarded as representative of the primitive materials from which the terrestrial planets formed. Results from the Viking organic analysis experiment place extremely low limits on the concentrations of volatile S compounds, including native and organic S, and many sulfide minerals (including pyrite) (*8*). The high level of S relative to the limits we have established for other elements also constrains the range of possible sulfur-containing compounds. Sulfides such as those of Cu, Zn, Pb, Hg, As, and Mo cannot be major components because of the demonstrated (Table 2)

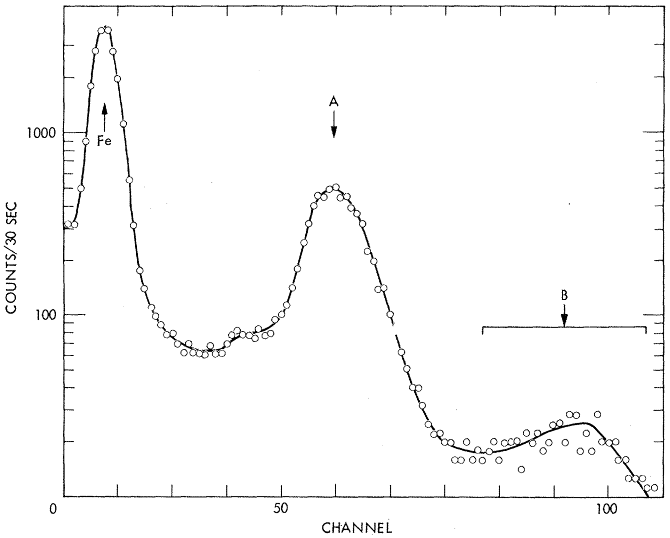

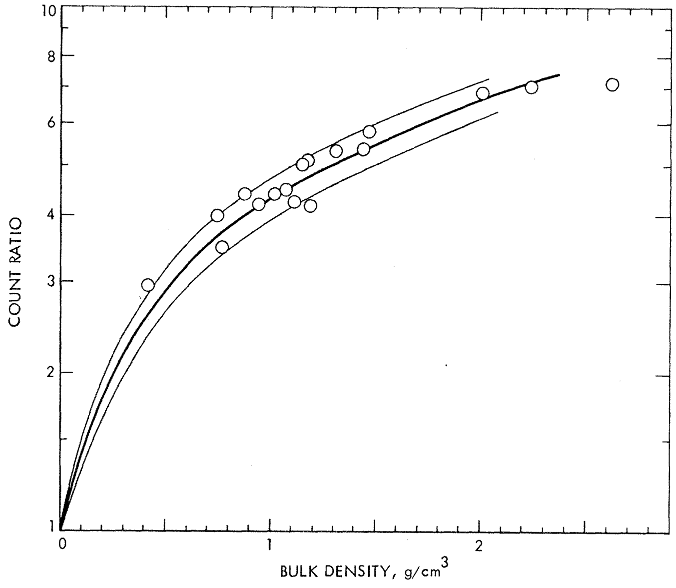

Fig. 2 (left). Data from detector PC3 on sample S1. Peak A represents the combined coherent and incoherent components of scattering of the 22.2-kev emission from the ^{109}Cd source. Peak B represents the incoherently scattered component of the 87.7 kev source emission, detected as the Xe escape peak; this is the peak used for the bulk density determinations. Fig. 3 (right). Calibration curve for bulk density determinations. The ordinate is the number of counts in peak B normalized to a set count in peak A. These data represent a composite of data from three instruments duplicating the geometry, sources, and detectors of the flight units. The thinner lines are the estimated error envelope.

low abundance of the required cations. Similarly, sulfates of K, Ba, Cu, or Pb cannot account for a significant fraction of the S present. Only sulfates of Na, Mg, Ca, and Fe, or sulfides of Fe (other than pyrite) can be regarded as candidate compounds. If a single sulfur compound were predominant, stoichiometric relationships would require 4.4 percent Na by weight, or 2.3 percent Mg, 3.9 percent Ca, or from 4.9 to 5.4 percent Fe. Thus, S could combine with all of the Ca, much of the Mg, or as much as one-third of the Fe present. Although we cannot directly determine Na, the presence of as much as a few percent seems unlikely considering the paucity of other alkalis (K, Rb) in the sample.

Potassium and argon. This experiment has established upper limits for both Ar in the martian atmosphere (*9*) and K in the soil. Measurements by mass spectrometer place the ^{40}Ar content at 1.6 percent by pressure (*10*). This is equivalent to 0.25 g/cm^2 for a mean Mars pressure of 6.0 mb; or a total atmospheric inventory of 3.7×10^{17} g, about 0.6 percent of the ^{40}Ar content of Earth's atmosphere (*5*). If one assumes that Mars has the same bulk K concentration as Earth and scales for the mass difference, this can be interpreted as implying a degree of degassing for Ar some 20 times lower on Mars than Earth. Based upon our K determination, we can suggest an alternative or supplementary basis for the difference. The average K content in the earth's crust is estimated at 1.25 to 2.1 percent (*11*). If the K content of <0.25 percent in the martian fines represents the average crustal material, there is at least 5 to 8 times less K near the surface for outgassing. Thus, if atmospheric ^{40}Ar correlates with average crustal K content, the relative deficiency of K-rich, and hence ^{40}Ar-rich, material near the surface is as significant as any postulated difference in overall outgassing.

Iron oxide coatings. We reported (*2*) that if the red to orange pigmenting agent in the fines were a thin coating of goethite or hematite over mineral grains, as proposed from studies of ground-based infrared reflection spectra from Mars (*12*), such a coating would have to be less than 1 to 2 μm thick, or discontinuous, because the low-energy x-ray from Mg has been detected. With the analytical results of Table 1 we can further restrict

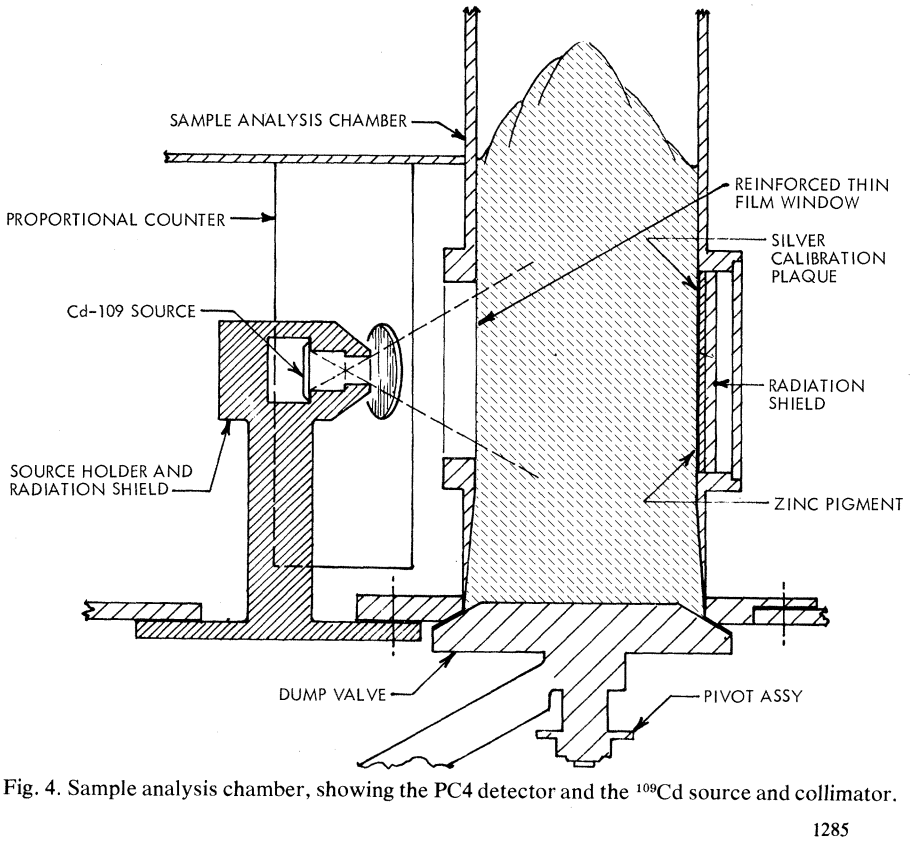

Fig. 4. Sample analysis chamber, showing the PC4 detector and the ^{109}Cd source and collimator.

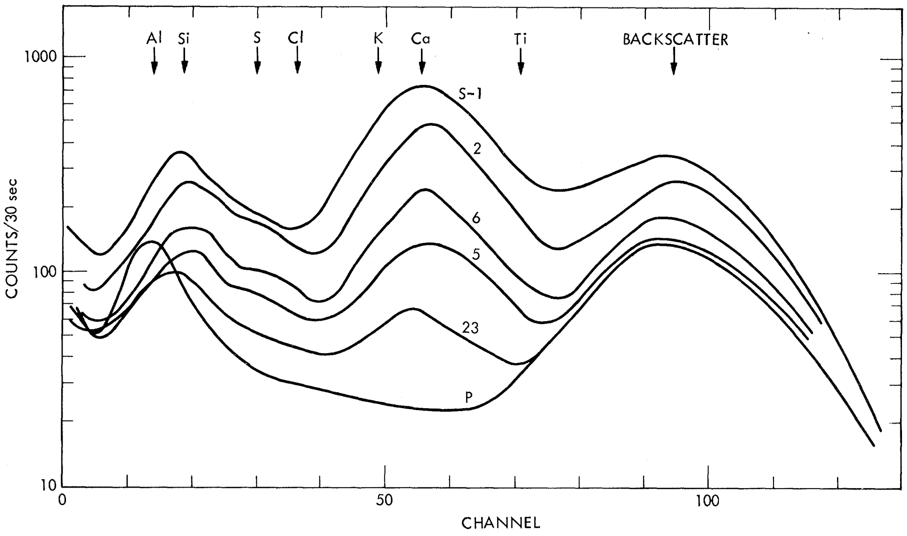

Fig. 5. Spectra taken with PC2 of an empty cavity immediately after landing (*P*), of the first sample (S1), and of various stages of sample purge. Note that after the sixth dump (6), the cavity was more contaminated than after the fifth (5), but by the time of the twenty-third purge (23) (that is, the ninth purge of S3; see Fig. 6), the cavity walls and windows were relatively, but not completely, clean.

this upper limit to 0.25 μm, because a coating thicker than this would attenuate x-rays from Mg, Al, and Si so much that the corrected bulk analysis would sum considerably above 100 percent. This argument applies, of course, only to the mineral components containing Mg, Al, and Si. For example, a thin coating of hematite over magnetite grains, as suggested by Huguenin (*13*), would be indistinguishable from the magnetite itself by our instrument. Similarly, a mixture of hematite grains with silicate particles could not be distinguished from silicates discontinuously coated.

Bulk density. A measure of the bulk density of the material in the sample analysis chamber is provided by the intensity of backscattering of the 87.7 kev nuclear gamma rays emitted by the ^{109}Cd source. For the XRFS geometry, this peak is Compton-shifted to 69.7 kev and detected by PC3 chiefly as the Xe escape peak (Fig. 2). A calibration curve on a variety of fine-ground and natural soils, including clays rich in iron, is shown in Fig. 3. From this, the bulk density of the S1 sample is determined as 1.10 ± 0.15 g/cm^3, a value at the low end of the range previously estimated by the Viking physical properties team (*14*). The range of possible mineralogical compositions consistent with the elemental analysis of Table 1 restricts the average mineral density to between 2.3 and 3.2 g/cm^3. This implies a bulk porosity of 60 ± 15 percent for the wind-drifted fines after delivery to the XRFS instrument (that is, after they have sifted through a 2-mm screen and fallen a distance of 25 cm through the inlet tube into the sample analysis chamber). This density may be comparable to that in the natural state because no artificial compaction is employed during delivery.

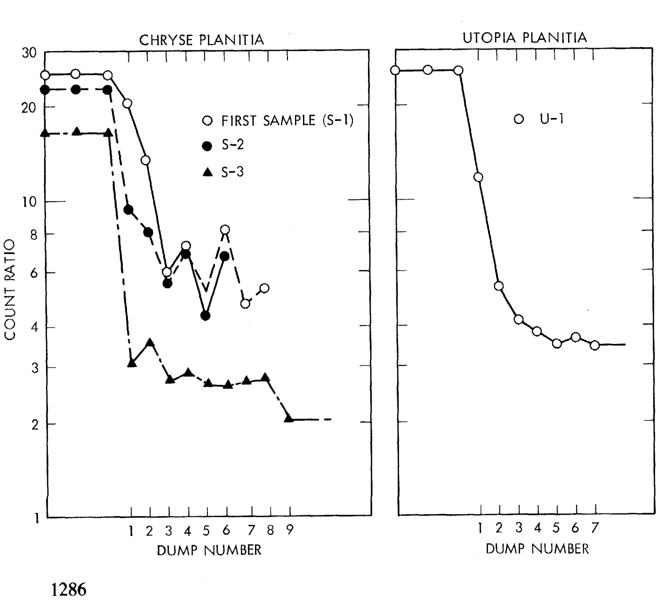

Fig. 6. Counts in the calcium peak region (3.2 to 4.5 kev), normalized to the spectrum of an empty analysis chamber (plaque spectrum), as a function of dump number for each sample.

Dump of sample 1. On the 31st martian day (sol 31) after the landing of Viking 1, the first of six purge sequences was initiated in order to empty and clean the chamber for receipt of the second sample. Each sequence consists of operating a spring-loaded trap door at the bottom of the sample analysis chamber (Fig. 4) at a rate of 4 hz for a total of 244 open-close cycles. Each closure produces an impact on the base of the chamber, which tends to dislodge dust adhering to the windows and calibration plaques. Prior to the landing, it was estimated from laboratory tests with fine-ground basalts and montmorillonite clays, for example, that six such sequences would provide adequate cleaning action. However, the martian fines at Chryse apparently exhibit stronger adhesion characteristics than any of the laboratory analogs tested. Sample spectra are shown in Fig. 5 for the PC2 detector, whose Ca peak is particularly sensitive to residual contamination inasmuch as no "interfering" calibration peaks are present. Figure 6 shows graphs of the integrated intensity of this peak. Three phenomena deserve special comment. First, as Fig. 6 shows, most even-numbered purge sequences for dumping samples S1 and S2 showed an actual increase of the Ca peak intensity rather than the expected decrease. These sequences had all been programmed to occur at about 2300 hours local lander time (L.L.T.), while the odd-numbered sequences occurred at about 1700 hours. A possible explanation of the oscillatory phenomenon is the preferential release of additional material trapped on the wind-spoiler flaps of the delivery funnel (Fig. 7) during periods of low atmospheric temperature. Second, comparisons of dump spectra with laboratory simulations indicate a somewhat disproportionate reduction of certain components in the spectra, with S and Cl becoming enriched. By analogy with common rock-forming minerals on Earth, it is likely that Si, S, Cl, and Ca are separately bound in at least two, and possibly four, distinct mineral phases. Third, from the determined composition and bulk density of the fines, the half-thicknesses for transmission of the calibration x-rays, Al Kα, Ag Lα, Mn Kα, and Zn Kα lines, can be calculated as 4, 12, 67, and 105 μm, respectively.

The first two components remained relatively obscured even after repeated dumps, consistent with there being a dust coating on the calibration plaques some ten or more micrometers thick. Laboratory observations of sample cavity contamination following purges of fine material show that the metallic plaques (and chamber walls) retain much more dust than do the thin film polycarbonate and polyimide windows.

Samples 2 and 3 at Chryse. On sol 34, the Viking 1 sampling scoop obtained material from an area dubbed "Rocky Flats" because of its concentration of pebble-sized fragments. The acquisition was programmed to obtain and deliver these fragments by means of a special surface sampler sequence (*4*) which included a 60-second sieve operation to remove fines. A 1.2-cm square grid in the XRFS funnel prevents entrance of larger fragments which might clog the 2.5-cm diameter delivery tube. Several characteristics of the spectra indicated that this sample (S2) filled the chamber at least to the height of the viewing windows; that is, the backscatter peaks were at full intensity and no evidence of calibration signals, including Zn, was present. If the average volume per fragment was 0.5 cm^3, then at least 25 fragments were delivered. The analysis spectra were remarkably similar to those of the fines, but the bulk density was measured at 0.6 ± 0.1 g/cm^3. If one assumes a void volume of the order of 50 percent, the density of the fragments themselves would be about 1.2 g/cm^3, that is, much less than that expected for a consolidated rock. After a short analysis, it was decided to dump this sample and repeat the acquisition sequences, this time with a 90-second sieving operation to improve the removal of any adhering dust. The third sample (S3) gave very similar results to S2, except that this time the total amount delivered was only 15 to 20 cm^3, as indicated by a weak but discernible Zn contribution in the spectra and an effective bulk density of only 0.4 g/cm^3, reflecting incomplete filling of the chamber. The amount present was sufficient to permit satisfactory analysis, although careful simulations will be necessary to derive final corrections, especially for ^{55}Fe contributions to the Fe peak and possible effects on trace element concentrations.

Comparison of Chryse samples. The measurement precision of the Viking XRFS instrument is considerably superior to its absolute accuracy for each element (*1*). Comparative measurements between similar samples, therefore, define elemental concentration trends more ac-

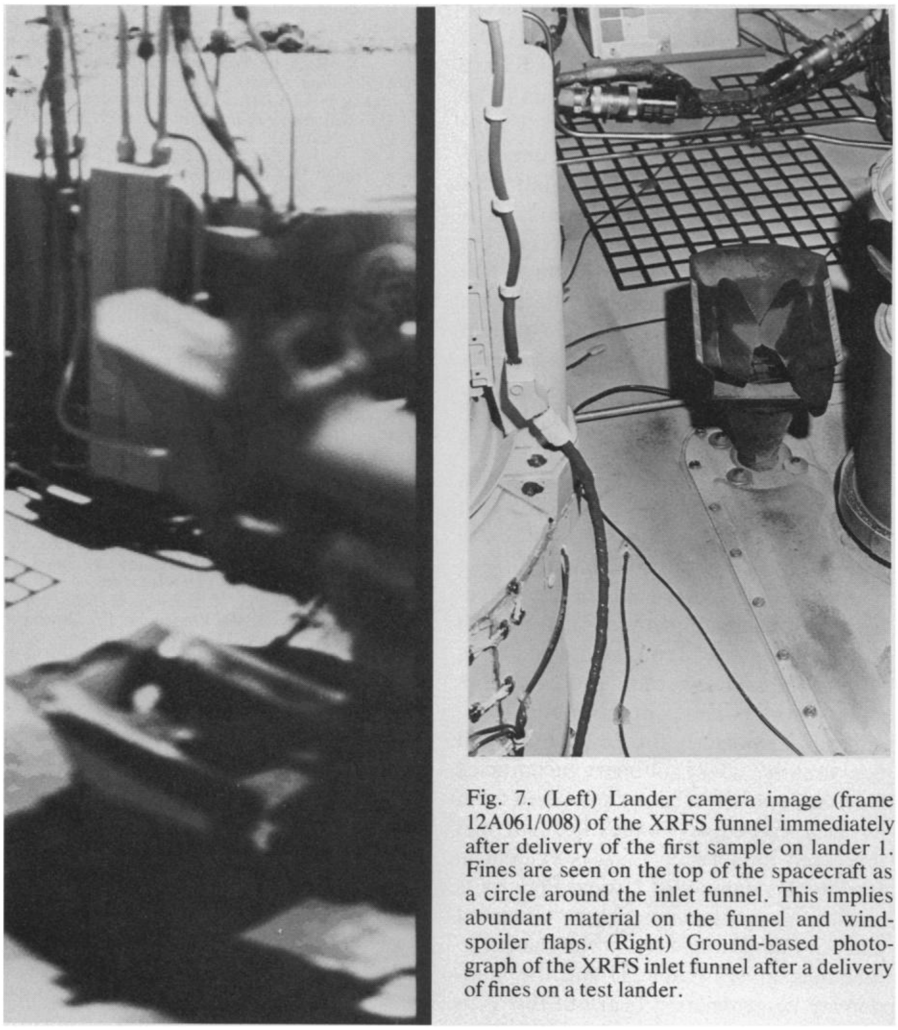

Fig. 7. (Left) Lander camera image (frame 12A061/008) of the XRFS funnel immediately after delivery of the first sample on lander 1. Fines are seen on the top of the spacecraft as a circle around the inlet funnel. This implies abundant material on the funnel and wind-spoiler flaps. (Right) Ground-based photograph of the XRFS inlet funnel after a delivery of fines on a test lander.

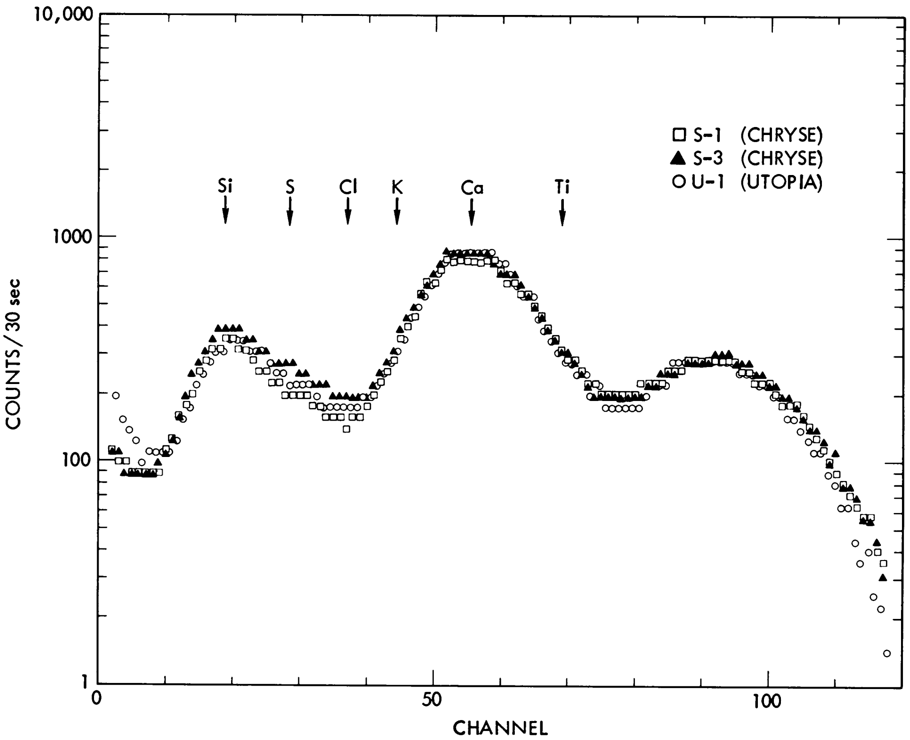

Fig. 8. Pooled spectra taken with detector PC2 on three Mars samples. Background subtractions and gain adjustments have been made to facilitate the comparison.

curately than absolute abundances. This capability is fully utilized for the Chryse suite of samples. In Table 1, note that the differences between S1, S2, and S3 are trivially small for many elements. The best-established difference is in S content, which increases by nearly one-half from S1 to S3. Sympathetic variation of other elements with the S increase is obviously difficult to establish, but the most likely candidate (excluding Na) seems to be Mg. Magnesium sulfate, or a hydrate thereof, could be an excellent cementing agent (*15*), and the fragments analyzed in S2 and S3 may therefore simply be fragments of a duricrust (*4*).

Utopia sample (U1). Within hours after the landing of the Viking 2 spacecraft, a calibration sequence of the XRFS unit was initiated. The data showed extra counts in some of the low channels. As a countermeasure, the gains of the detectors have been commanded high enough to place all peaks required for analyses above channel 24. Data reduction becomes more complex in this mode of operation, particularly for PC1, but should not greatly affect ultimate accuracies (*16*). Sample U1 was of fines taken from an area known as Bonneville, and was delivered on sol 29 (*4*). As is evident in Fig. 8, this sample at Utopia Planitia is strikingly similar to those taken at Chryse Planitia, and the preliminary elemental analysis (Table 1) and the bulk-density determination bear out this generalization. The implications of this finding and the mineralogic and petrologic interpretations of our results are discussed elsewhere (*4*).

BENTON C. CLARK
Planetary Sciences Laboratory,
Martin-Marietta Aerospace,
Denver, Colorado 80201
A. K. BAIRD
Department of Geology,
Pomona College,
Claremont, California 91711
HARRY J. ROSE, JR.
PRIESTLEY TOULMIN III
U.S. Geological Survey,
Reston, Virginia 22092
KLAUS KEIL
Department of Geology and *Institute of Meteoritics, University of New Mexico,*
Albuquerque, 87123
ANGELO J. CASTRO
Martin-Marietta Aerospace
WARREN C. KELLIHER
NASA Langley Research Center,
Hampton, Virginia 23665
CATHERINE D. ROWE
Martin-Marietta Aerospace
PETER H. EVANS
Department of Geology,
Pomona College

References and Notes

1. P. Toulmin III, A. K. Baird, B. C. Clark, K. Keil, H. J. Rose, Jr., *Icarus* **20**, 153 (1973); B. C. Clark, A. K. Baird, P. Toulmin III, H. J. Rose Jr., K. Keil, in *Nuclear Methods in Minerals Exploration.*, J. G. Morse, Ed. (Elsevier, in press); B. C. Clark and A. K. Baird, *Geology* I, 15 (1973); *Earth Planet. Sci. Lett.* **19**, 359 (1973).
2. P. Toulmin III, B. C. Clark, A. K. Baird, K. Keil, H. J. Rose, Jr., *Science* **194**, 81 (1976).
3. R. Hanel, B. Conrath, W. Hovis, V. Kunde, P. Lowman, W. Maguire, J. Pearl, J. Pirraglia, C. Prabhakara, B. Schlachman, G. Levin, P. Straat, T. Burke, *Icarus* **17**, 423 (1972).
4. A. K. Baird, P. Toulmin III, B. C. Clark, H. J. Rose, Jr., K. Keil, R. P. Christian, J. L. Gooding, *Science* **194**, 1288 (1976).
5. B. Mason, *Principles of Geochemistry* (Wiley, New York, 1958).
6. C. W. Field, in *Encyclopedia of Geochemistry and Environmental Sciences IVA*, R. W. Fairbridge, Ed. (Van Nostrand Reinhold, New York, 1972).
7. S. R. Taylor, *Lunar Science: A Post-Apollo View* (Pergamon, New York, 1975).
8. K. Biemann, J. Oro, P. Toulmin III, L. E. Orgel, A. O. Nier, D. M. Anderson, P. G. Simmonds, D. Flory, A. V. Diaz, D. R. Rushneck, J. A. Biller, *Science* **194**, 72 (1976).
9. B. C. Clark, P. Toulmin III, A. K. Baird, K. Keil, H. J. Rose, Jr., *ibid.* **193**, 804 (1976).
10. T. Owen, private communication; T. Owen and K. Biemann, *Science* **193**, 801 (1976).
11. K. S. Heier and G. K. Billings, in *Handbook of Geochemistry*, K. H. Wedepohl, Ed. (Springer-Verlag, New York, 1970), vol. 2, part 2.
12. A. B. Binder and D. P. Cruikshank, *Icarus* **5**, 521 (1966); J. W. Salisbury and G. R. Hunt, *Science* **161**, 365 (1968); *Nature (London)* **222**, 132 (1969); J. B. Adams and T. B. McCord, *J. Geophys. Res.* **74**, 4851 (1969); A. B. Binder and J. C. Jones, *ibid.* **77**, 3005 (1972).
13. R. L. Huguenin, *J. Geophys. Res.* **79**, 3895 (1974).
14. R. W. Shorthill, H. J. Moore, II, R. F. Scott, R. E. Hutton, S. Liebes, Jr., C. R. Spitzer, *Science* **194**, 91 (1976).
15. Laboratory preparation of geochemical analog materials has shown that silt-sized rock particles can be firmly cemented together by evaporation of water from samples which have been soaked in aqueous solutions of $MgSO_4$ to produce a sample containing about 3 percent S by weight. The resultant coarse aggregrates are sufficiently coherent to withstand the acquisition, sieve, and delivery operations by Viking surface sampler.
16. All XRFS spectra obtained on Viking 2 since it landed have shown spurious pulses in the lowest 24 of the 128 channels into which each spectrum is analyzed. The noise is present in all four detectors but is more pronounced for PC1 and PC4 than for the other two. Special test sequences on sols 10, 14, 16, 17, and 27 included the operation of the detectors at essentially zero gain so that only electronic noise bursts were detected, and the results showed clearly that the noise detected by the XRFS was directly correlated with activity of the on-board guidance, control, and sequencing computer (GCSC). Because the noise is restricted to the lower part of each spectrum, the most seriously affected determinations are those of Mg, Al, and Si. The noise occurs in the same channels, independent of detector gain, however, and the peaks corresponding to these elements can be shifted to noise-free parts of the spectrum by suitably increasing detector gain. This causes the backscatter peak to fall off scale, requiring indirect procedures for normalization and gain and offset calibration by comparison of data taken at high and at nominal gains.
17. We are indebted to the people responsible for the design, development, and manufacture of the XRFS flight instruments. We acknowledge at Martin-Marietta, builder of the XRFS, T. Allen, W. W. Bender, A. Castro, D. Reinhardt, and J. Sterhardt in management; D. Barnett, W. Crissey, R. Czarnecki, M. Mason, R. Moore, W. Rintella, W. Starkey, D. Stout, and C. Wilkerson, engineering; R. Berry, R. Card, D. Johnson, J. Leonard, R. Mish, J. Motter, H. Over, J. Peterson, W. Schumacher, and A. Wells in manufacturing and test. We also thank the employees of Reuter-Stokes, manufacturer of the detectors; Isotope Products Laboratories, supplier of the radiation sources; and R. M. Ely at NASA Langley Research Center for supplying the polyimide film for sample cavity windows. For assistance with data reduction we thank the Science Interns: R. Weldon of Pomona College, B. Sawhill of Stanford University, K. Molenaar of Gustavus Adolphus College, K. Brau of Harvard University, R. Wall of U.S. Naval Academy, and for the laboratory assistance we thank S. Kenley of Martin-Marietta. R. B. Hargraves kindly reviewed this manuscript. This work was supported in part by NASA (Viking Program) grants NAS 1-11855, NAS 1-11858, L-9717, and NAS 1-9000.

15 November 1976

Mineralogic and Petrologic Implications of Viking Geochemical Results From Mars: Interim Report

Abstract. *Chemical results from four samples of martian fines delivered to Viking landers 1 and 2 are remarkably similar in that they all have high iron; moderate magnesium, calcium, and sulfur; low aluminum; and apparently very low alkalies and trace elements. This composition is best interpreted as representing the weathering products of mafic igneous rocks. A mineralogic model, derived from computer mixing studies and laboratory analog preparations, suggests that Mars fines could be an intimate mixture of about 80 percent iron-rich clay, about 10 percent magnesium sulfate (kieserite?), about 5 percent carbonate (calcite), and about 5 percent iron oxides (hematite, magnetite, maghemite, goethite?). The mafic nature of the present fines (distributed globally) and their probable source rocks seems to preclude large-scale planetary differentiation of a terrestrial nature.*

Both Viking landers (VL) are in relatively low, basinal areas of Mars (VL1 at Chryse Planitia and VL2 at Utopia Planitia) characterized by abundant red-colored fine material and scattered blocks of generally angular rocks. At the site of VL1 there is more geologic diversity than at the VL2 site: pitted and relatively unpitted rocks, both light and dark colored; abundant dunelike deposits; and outcrops of apparent bed rock, crudely layered and perhaps intruded by a dike (*1*). The VL2 site, by contrast, is a flat plain more densely covered with angular blocks of uniformly dark-colored, pitted, fine-grained rocks. At both sites, but more prominently at VL2, the uppermost surface of fine material appears to be cemented into a crust 1 to 2 cm thick, which seems to range widely in mechanical strength. As of this report, four samples (three at VL1 and one at